MICROFLARE ACTIVITY DRIVEN BY FORCED MAGNETIC RECONNECTION

2010 ApJ 712 L111

(http://iopscience.iop.org/2041-8205/712/1/L111)

The Astrophysical Journal Letters, 712:L111–L115, 2010 March 20 doi:10.1088/2041-8205/712/1/L111

MICROFLARE ACTIVITY DRIVEN BY FORCED MAGNETIC RECONNECTION

D. B. Jess[1], M. Mathioudakis[1], P. K. Browning[2], P. J. Crockett[1], and F. P. Keenan[1]
[1] Astrophysics Research Centre, School of Mathematics and Physics, Queen's University, Belfast, BT7 1NN, UK; d.jess@qub.ac.uk
[2] Jodrell Bank Centre for Astrophysics, School of Physics and Astronomy, University of Manchester, Manchester, M13 9PL, UK
Received 2009 November 20; accepted 2010 February 19; published 2010 March 5

ABSTRACT

High cadence, multiwavelength, optical observations of a solar active region, obtained with the Swedish Solar Telescope, are presented. Two magnetic bright points are seen to separate in opposite directions at a constant velocity of 2.8 km s^{-1}. After a separation distance of ≈4400 km is reached, multiple Ellerman bombs are observed in both Hα and Ca-K images. As a result of the Ellerman bombs, periodic velocity perturbations in the vicinity of the magnetic neutral line, derived from simultaneous Michelson Doppler Imager data, are generated with amplitude ±6 km s^{-1} and wavelength ≈1000 km. The velocity oscillations are followed by an impulsive brightening visible in Hα and Ca-K, with a peak intensity enhancement of 63%. We interpret these velocity perturbations as the magnetic field deformation necessary to trigger forced reconnection. A time delay of ≈3 minutes between the Hα-wing and Ca-K observations indicates that the observed magnetic reconnection occurs at a height of ∼200 km above the solar surface. These observations are consistent with theoretical predictions and provide the first observational evidence of microflare activity driven by forced magnetic reconnection.

Key words: Sun: activity – Sun: atmosphere – Sun: chromosphere – Sun: evolution – Sun: flares – Sun: photosphere

Online-only material: animation

1. INTRODUCTION

Magnetic reconnection is a common phenomenon within the solar atmosphere. Its presence is often observed through explosive events such as solar flares, where extreme localized heating is generated through the conversion of magnetic energy (Priest 1986). Forced magnetic reconnection is a type of reconnection process which allows a fast transition of the magnetic configuration to a state of lower energy (Vekstein & Jain 1998). In this regime, it is believed that the displacement of photospheric footpoints deforms the initially smooth magnetic field configuration, generating a current sheet and forcing reconnection (Jain et al. 2005). This form of reconnection is often modeled by implementing a sinusoidal boundary disturbance to a slab plasma with a field reversal, which drives the formation of a current sheet and causes reconnection at the magnetic neutral line (Ma et al. 1996).

Observational evidence of magnetic reconnection occurring in the lower solar atmosphere (photosphere and chromosphere) is rare. It is generally assumed that reconnection and the subsequent release of magnetic energy is a coronal process, often occurring many thousands of kilometers above the surface of the Sun. However, in recent years Ding et al. (1999) and Chen et al. (2001) have provided evidence of eruptive phenomena and localized heating in the lower solar atmosphere, through the analysis of type II white-light flares and Ellerman bombs. Unfortunately, for these cases there are currently no available theoretical models that can deal with the particle acceleration created. Indeed, since the surrounding plasma is much denser than in the corona, partially ionized and highly collisional, it is believed that most of the energy released through magnetic reconnection is promptly consumed (Chen & Ding 2006). To date, there has been no observational evidence of flare activity driven by forced reconnection.

Theoretically, it was noted by Roumeliotis & Moore (1993) that reconnection could proceed rapidly in the photosphere due to the low conductivity of cooler plasmas, and this was used to interpret canceling magnetic features as photospheric reconnections. This idea was further developed by Litvinenko (1999) and Litvinenko et al. (2007). However, the models presented are based on, respectively, oscillatory reconnection and steady-state Sweet Parker reconnection, which do not appear appropriate for transient events. In addition to the characteristic lower temperatures, reconnection in a partially ionized photosphere may be distinguished from more commonly studied coronal reconnection by the interactions with neutrals. A few theoretical studies have tackled the question of reconnection in a partially ionized plasma (e.g., Bulanov & Sakai 1998), but the process remains poorly understood.

The data presented here are part of an observing sequence obtained on 2007 August 24 with the Swedish Solar Telescope (SST) on the island of La Palma. Our optical setup allowed us to image a 68″ × 68″ region surrounding active region NOAA 10969 complete with solar rotation tracking. This active region was located at heliocentric coordinates (−516″, −179″), or S05E33 in the solar NS-EW coordinate system. The Solar Optical Universal Polarimeter was implemented to provide two-dimensional spectral information across the Hα line profile centered at 6562.8 Å. In addition, a series of Ca II interference filters were used to provide high-cadence imaging in this portion of the optical spectrum. The observations and data reduction employed in the present analysis are described in detail by Jess et al. (2008). For the purpose of this Letter, two-dimensional Hα spectral scans, Ca K core, and blue (Ca II) continuum observations will be presented, along with full-disk Michelson Doppler Imager (MDI; Scherrer et al. 1995) magnetograms which are used to evaluate magnetic neutral line locations. During the observing sequence, a microflare event was observed, originating southeast of NOAA 10969 at 08:42 UT.

Traditional microflares are defined as transient bursts, which release energy into the surrounding solar plasma over timescales normally less than 10 minutes (Krucker et al. 2002). These bursts, classified as low *GOES* C class to below A class events, frequently produce hard X-rays as a result of bremsstrahlung

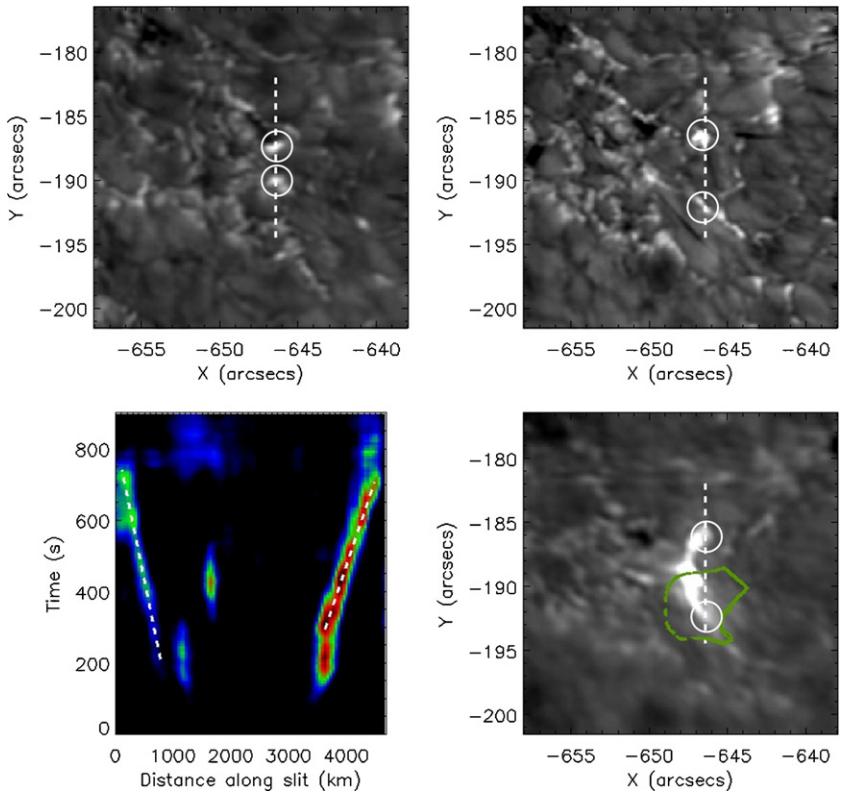

Figure 1. Top left: separation of the MBPs at 08:28 UT. Top right: greater MBP separation observed at 08:38 UT. White circles mark the expected position of the footpoints, and the dashed white lines indicate the slit position used to establish velocities. Lower left: time–distance plot demonstrating the observed separation of the MBPs as a function of time. The dashed white lines indicate a least-squares fit to the slopes, with the gradient providing the velocity for each MBP. The gradient observed indicates the presence of constant separation velocities, evaluated to be 1.0 km s^{-1} and 1.8 km s^{-1} for the left (most northerly) and right (most southerly) MBPs, respectively. Lower right: Hα microflare event, observed at the time of peak emissive flux (08:42 UT), with green contours marking the location of the magnetic neutral line. The brightest emission from the loop structure, seen to link the two MBPs, is cospatial with the underlying neutral line.

(An animation of this figure is available in the online journal.)

emission when non-thermal particles collide with the dense lower solar atmosphere (Hannah et al. 2008). Additionally, microflares are well correlated with large-scale solar activity, and as a result only occur in the vicinity of active regions (Christe et al. 2008). Therefore, while the term "microflare" is normally reserved for phenomena detectable in X-rays, on this occasion no such emission was established. However, due to consistencies with typical microflare characteristics (as will be discussed throughout), we deem this event an "Hα microflare." In this Letter, we utilize the high-cadence multiwavelength data set to search for definitive evidence of microflare activity in the lower solar atmosphere driven by forced reconnection.

2. ANALYSIS AND RESULTS

Prior to the Hα microflare event, two magnetic bright points (MBPs; Crockett et al. 2009) are observed at 08:28 UT to be separated by ≈2700 km at heliocentric coordinates (−646″, −188″), as indicated by the white circles in the upper panels of Figure 1. Over the next 10 minutes, the MBPs are observed in both the blue Ca II continuum and Hα-wing (core ± 700 mÅ) observations to diverge until they are separated by a distance exceeding ≈4400 km. The lower left panel of Figure 1 is a time–distance plot, obtained by placing a slit along the motion paths of the MBPs, revealing the displacement of these structures as a function of time. By establishing the gradient, and hence velocity, associated with the MBPs in the time–distance plot, as indicated by the dashed white lines in the lower left panel of Figure 1, it is clear that each MBP displays a constant separation velocity, equal to ≈1.0 km s^{-1} for the most northerly MBP and ≈1.8 km s^{-1} for the most southerly one. Due to the movement of the two MBPs in opposite directions, the net separation velocity equates to ≈2.8 km s^{-1}. This velocity is consistent with the measured separation distance over the 10 minute duration ($\frac{4400\,\mathrm{km} - 2700\,\mathrm{km}}{600\,\mathrm{s}} = 2.83$ km s^{-1}) and reiterates the presence of a constant separation velocity in opposing directions.

The maximum MBP separation distance of ≈4400 km is achieved at 08:38 UT. During the next 4 minutes, both MBPs remain stationary and exhibit no fluctuations in their observed size. However, during this time, line-of-sight velocity oscillations are created along a curved path linking the two MBPs (the upper left panel of Figure 2). These photospheric velocities are derived from 36 s cadence Doppler shifts of the Hα line bisector positioned at ±700 mÅ from the core of a rest Hα profile, and constitute four complete periods with amplitude ±5 km s^{-1} and wavelength ≈1000 km. However, due to the telescope pointing being directed away from the center of the solar disk, the $\cos\theta \approx 0.8$ angle must be taken into consideration when determining absolute velocities. Since MBPs in the photosphere often show negligible inclination angles to the solar surface (Sanchez Almeida & Martinez Pillet 1994), incorporation of the viewing angle provides an absolute velocity amplitude of ±6 km s^{-1} normal to the solar surface. Furthermore, simultaneous Doppler velocities are also established using the methods detailed in Suematsu et al. (1995), providing a Doppler map, *Dopp*, given by $Dopp = (C_b - C_r)/(C_b + C_r + 2)$, where C_b and C_r are contrast images obtained using the relation $C = (I - I_a)/I_a$. I_a corresponds to the average intensity over the entire data set,

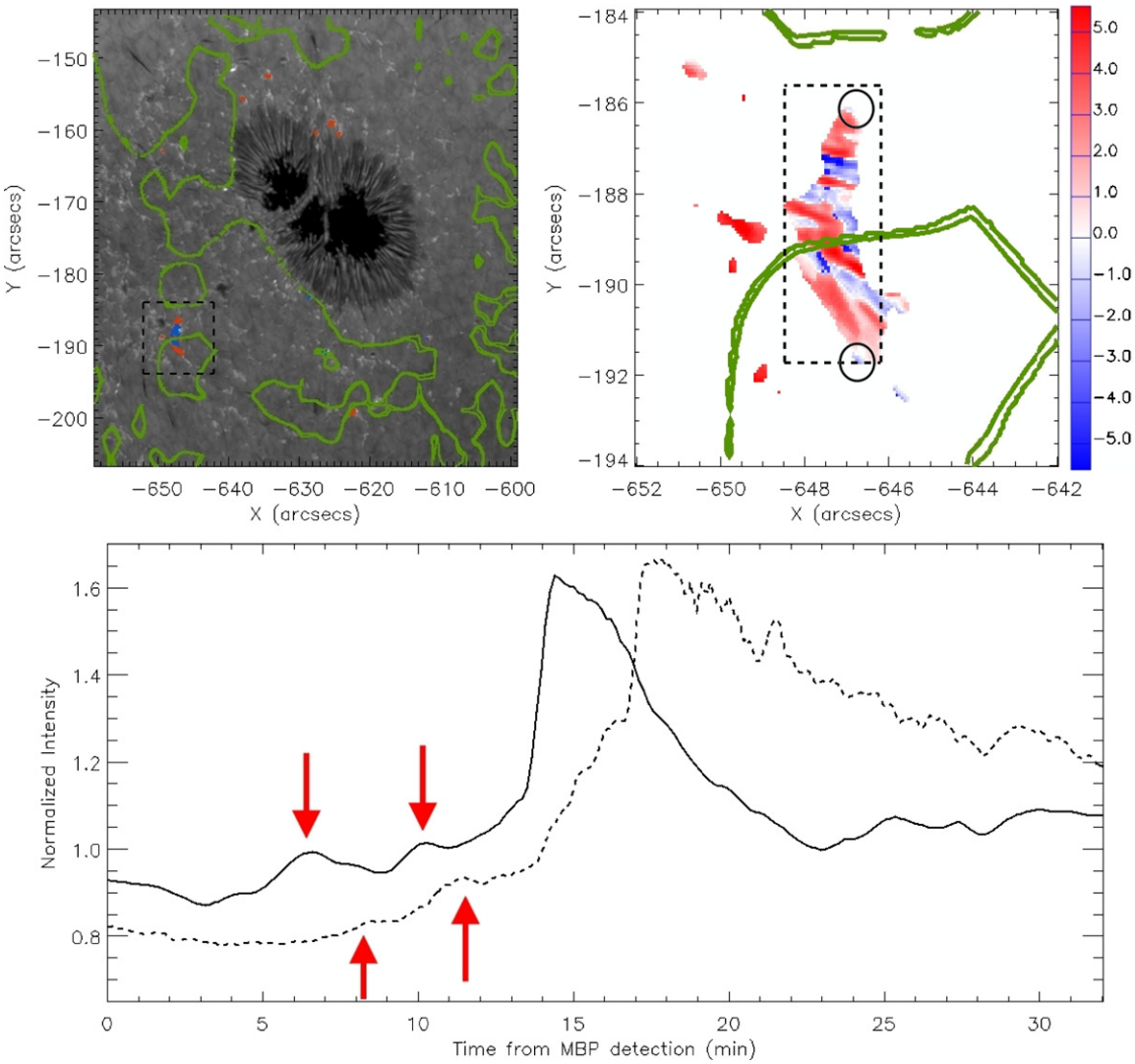

Figure 2. Upper left: Hα blue-wing (Hα-core −700 mÅ) field of view overplotted with velocity contours exceeding ±3 km s^{-1}. Red contours indicate red-shifted Doppler velocities; blue contours indicate blue-shifted Doppler velocities; and green contours mark the locations of the magnetic neutral line. The dashed black lines mark a region which is magnified in the upper right panel. Upper right: Doppler map obtained from difference imaging at Hα-core ±700 mÅ wavelengths. The color table indicates derived velocities in km s^{-1}, while the black circles mark the expected location of the magnetic field footpoints shown in Figure 1. Bottom: normalized intensity (Hα wing: solid line; Ca-K: dashed line) plotted as a function of time. Each intensity value is an average derived from within the box outlined by the dashed black lines in the upper right panel. Intensity fluctuations in the minutes prior to the Hα microflare are consistent with observations of Ellerman bombs (indicated by red arrows).

while the subscripts *b* and *r* correspond to the wavelengths at Hα-core −700 mÅ and Hα-core +700 mÅ, respectively. These Doppler maps also reveal an identical velocity oscillation characterized by an amplitude of ±5 km s^{-1} (±6 km s^{-1} with viewing-angle correction) and a wavelength of ≈1000 km (the upper right panel of Figure 2). It is interesting to note that the velocity oscillation crosses the path of the magnetic neutral line derived from full-disk MDI magnetograms. Theoretical modeling by Vekstein & Bian (2005) has shown how quasi-static perturbations to an initially stable magnetic field configuration may induce magnetic reconnection at the system's neutral X-point. Indeed, Vekstein & Jain (1998) have shown that even a weak external deformation of the magnetic field lines can produce a substantial magnetic relaxation. As a result, flare sites are often observed to coincide with the magnetic neutral line (Ding et al. 2003; Jess et al. 2008).

What exactly causes a deformation of the magnetic field lines is open to interpretation. It has been suggested that Ellerman bombs (Ellerman 1917), which occur at the footpoints of magnetic loops (Denker et al. 1995), may trigger bidirectional velocity disturbances in regions of weak fluxes of mixed polarity (Chae et al. 1998). Observations of such phenomena have recently been presented by Madjarska et al. (2009), where the reported observational signatures of Ellerman bombs include symmetric intensity enhancements (rise and decay times are approximately equal), and numerous up- and down-flows detected in the wings of the Hα profile. Typical sizes of Ellerman bombs are ≈1″–2″ in diameter (Nindos & Zirin 1998) and they evolve with lifetimes in the range 4–20 minutes (Denker et al. 1995). Furthermore, Qiu et al. (2000) suggest that these events evolve with a phase difference between photospheric and chromospheric observations as a result of upward-moving plasma, triggered by the Ellerman bomb at a height of <350 km.

From the lower panel of Figure 2, it is clear that repeated Hα-wing intensity enhancements are visible in the lead up to the Hα microflare event. Using an integration area defined by the

dashed black lines in the upper right panel of Figure 2, these intensity fluctuations provide a symmetric profile enhancement of ≈12% to the background quiescent flux. This is consistent with previous measurements related to Ellerman bombs, where Georgoulis et al. (2002) detect intensity enhancements of ≈5%–30%. However, if the integration areas are modified so that only the flux of the MBPs are considered, the intensity enhancements increase dramatically to ≈43%, higher than reported in Zachariadis et al. (1987). This larger intensity contrast may be a result of the high spatial resolution of our data, which allows fine-scale structures to be resolved without the intensity-smearing associated with less-favorable spatial resolution. Furthermore, the physical sizes of the MBPs are ≈1″ in diameter, remaining consistent with the dimensions of typical Ellerman bomb sites (Nindos & Zirin 1998). The MBPs associated with Ellerman bomb locations are often observed to exhibit proper motions parallel to the surface of the Sun (Denker 1997). These motions can frequently exceed 1 km s^{-1} in regions surrounding sunspots (Georgoulis et al. 2002). The lower left panel of Figure 1 demonstrates a proper motion of 1–1.8 km s^{-1} for the MBPs under investigation. Thus, we deem these symmetric intensity fluctuations visible in the lower panel of Figure 2 to be the signature of Ellerman bombs, which generate the periodic velocity perturbations observed along the loop structure. In addition, it has been suggested that the production of such bidirectional velocity flows may act as a precursor to the presence of magnetic reconnection (Dere 1994). It should be noted that the periodic velocity perturbations evaluated here correspond to significant blue and red shifts (±6 km s^{-1}) of the Hα line profile bisectors, yet remain below the sound speed in the photosphere.

An important parameter for forced reconnection is the magnitude of the driving displacement, δ. This is the maximum distance by which the boundary is perturbed. Forced reconnection can take place in various configurations, but assuming the simplest scenario of reconnection occurring along the vertical field above a neutral line, the relevant displacement is horizontal. In this example, the average horizontal velocity is estimated to be ≈7 km s^{-1}, which, over a 4 minute time interval, gives a displacement of about 1600 km. Comparing this with the separation distance of 4400 km gives a normalized displacement $\delta/a \approx 1/3$. As a result, forced reconnection is expected to be strong and nonlinear.

At 08:42 UT, the periodic velocity perturbation linking the two MBPs gives way to a substantial Hα microflare event, visible in both the Hα-wing and Ca-K data sets. The flare ribbon directly links the two MBPs and closely outlines the location of the velocity oscillation observed immediately prior to the Hα microflare (the lower right panel of Figure 1). Typically, reconnection sites originate in locations of strong magnetic field gradient, where the field strength changes abruptly over a very short distance. Thus, we believe that where a significant intensity enhancement of 63% above the quiescent mean (peak intensity from lower panel in Figure 2) is found and a cospatial magnetic neutral line is observed, is the location where forced magnetic reconnection occurs. An intensity enhancement of 63% is consistent with previous microflare observations and theoretical predictions (Hudson 1991; Jess et al. 2007).

As predicted by Qiu et al. (2000), we utilize the high-temporal resolution of our data set (Hα = 9 s; Ca-K = 2.5 s) to determine a clear phase shift in the light curves generated for photospheric (Hα wing) and lower chromospheric (Ca-K) observations. A time delay of ≈3 minutes is visible in the lower panel of Figure 2, and applies to both the signatures of Ellerman bombs (visible at times of 6.5 minutes and 10 minutes in the Hα-wing light curve) and the Hα microflare event (at a time of 14 minutes in the Hα-wing light curve). The Hα line-bisector velocities determined at the time of peak Hα microflare flux demonstrate values of ≈6 km s^{-1}. In the lower solar atmosphere where radiation is the dominant energy loss mechanism for flares (Emslie et al. 1981), magnetic reconnection often leads to isotropic heating of the plasma (Machado et al. 1989). Thus, we can use the Hα line-bisector velocities of ≈6 km s^{-1} as a good estimate of the flare-induced plasma velocity normal to the solar surface. As a result, for plasma traveling upward toward the layer of the solar atmosphere seen in Ca-K wavelengths (1200 km; Beebe & Johnson 1969), a time delay of ≈3 minutes and a velocity of ≈6 km s^{-1} provide a traversed distance of ≈1000 km. Subtracting this value from the formation height of Ca-K provides a reconnection altitude of ∼200 km above the solar surface, consistent with the formation height of the Hα wing (<300 km). In this regime, upward flowing, hot plasma, generated at the reconnection altitude of ∼200 km, is visible in Hα-wing observations (<300 km) immediately, before being detectable at Ca-K altitudes (≈1200 km), after a time delay of ≈3 minutes. This derived Hα microflare altitude is consistent with lower atmospheric reconnection models presented in Ding et al. (1999).

It is interesting to note that the Hα microflare intensity enhancements are not visible in the core of the Hα line. A possible interpretation may be the magnetic field lines connecting the two MBPs not reaching sufficiently high into the solar atmosphere to be seen in Hα-core observations. Another possibility, as noted by Chen & Ding (2006), is that the high densities found in the lower solar atmosphere, coupled with a partially ionized and highly collisional plasma, mean that any energy released through magnetic reconnection is promptly consumed, preventing accelerated plasma from traversing large distances as they would in the corona. With an Hα-core formation height of ≈1500 km (Vernazza et al. 1981), the lack of microflare signatures at this atmospheric height may be due to the hot plasma surrounding the reconnection site being rapidly cooled before it reaches these elevated altitudes.

The evolution of the Hα microflare continues over the next 9 minutes, during which the observed intensity gradually decays back to its quiescent value (see the lower panel of Figure 2). Three minutes after the initial impulsive phase of reconnection, an abundance of red-shifted plasma, particularly in locations surrounding the MBPs, is detected with velocities exceeding 6 km s^{-1} (7.5 km s^{-1} normal to the solar surface with viewing-angle correction). These downward velocity trends are consistent with Ding et al. (1995), who describe how downward mass motions appear near the extreme edges of flare ribbons.

Since, as discussed above, the forced reconnection is strongly driven, this may result in the nonlinear phase predominating. The characteristic timescale, τ_N, of nonlinear forced reconnection is, $\tau_N \equiv (\tau_0 \tau_R \tau_A^3)^{1/5}$ (Wang et al. 1996), where $\tau_0 = a/v_0$ is the driving timescale, $\tau_R = a^2/\eta$ is the resistive timescale with η, the magnetic diffusivity, defined as $\eta = 1/\mu_0\sigma$, and τ_A is the Alfvén timescale (a is the characteristic length scale of the initial current sheet and v_0 is the driving velocity). Adopting values corresponding to the above observations, i.e., $a \approx 4400$ km, $T \approx 5000$ K, $n = 2 \times 10^{21}$ m^{-3}, $B = 500$ G, and $\sigma = 7.4 \times 10^{-4} T^{3/2}$, we establish $\tau_N \approx 87$ minutes, assuming purely classical resistivity (Spitzer 1956). This is somewhat

longer than the observed reconnection timescale of about 9 minutes, although of the correct order of magnitude. However, the derived timescale is strongly dependent on the assumed current sheet length scale, a. If a is taken to be the gravitational scale height (following Litvinenko & Martin 1999), which is ∼100 km, a much more rapid reconnection timescale is obtained. Furthermore, any effects due to anomalous resistivity will also significantly reduce the reconnection timescale. The energy release associated with this event will scale as the total magnetic energy multiplied by $(\frac{\delta}{a})^2$ (Vekstein & Jain 1998), where δ, as mentioned above, is the magnitude of the boundary disturbance. Based on a loop of length 4000 km and diameter 725 km, this gives an order-of-magnitude energy release of 10^{22} J, which is consistent with previous studies of microflare energetics (e.g., Hannah et al. 2008).

This event has been classified as an Hα microflare, due to a lack of detectable X-ray emission. However, the impulsive nature of the Hα light curve, accompanied by its derived energy release, duration, occurrence at a magnetic neutral line, associated plasma acceleration, and correlation with solar activity, suggests that this phenomena may have more in common with typical X-ray microflares than first anticipated. A lack of detectable X-ray emission may simply be due to the reconnection process occurring deep within the lower solar atmosphere, where the associated energy release is promptly consumed, producing either no X-ray emission, or emission so faint that current satellites cannot detect it.

3. CONCLUDING REMARKS

The unprecedented spatial and temporal resolution data acquired with the SST have revealed a small-scale impulsive brightening in Hα and Ca-K, which we interpret as microflare activity driven by forced reconnection. A progressive separation of two MBPs, followed by a periodic velocity perturbation, results in magnetic reconnection at the location of a polarity inversion line. Multiple Ellerman bombs are observed in the vicinity of the MBPs using both Hα and Ca-K imaging, which are deemed to trigger periodic velocity oscillations along the loop structure connecting the MBPs. Bidirectional velocity perturbations created by the Ellerman bombs reveal amplitudes of ± 6 km s^{-1} and a wavelength of ≈1000 km. We interpret the generated velocity oscillations as the magnetic field deformation necessary to trigger forced reconnection, thus demonstrating how small-scale reconnection (e.g., from an Ellerman bomb) can trigger a larger reconnection event. Furthermore, the resulting magnetic reconnection occurs cospatially with the magnetic neutral line at an estimated atmospheric height of ∼200 km. Calculations suggest that the observed trends are best represented by forced reconnection models in a nonlinear regime, with an expected energy release of the order of 10^{22} J.

D.B.J. thanks STFC for a Post-Doctoral Fellowship. F.P.K. thanks AWE Aldermaston for the William Penney Fellowship. The SST is operated by the Institute for Solar Physics of the Royal Swedish Academy of Sciences. These observations have been funded by OPTICON, within the Research Infrastructures of FP6. This work is supported by EOARD.

REFERENCES

Beebe, H. A., & Johnson, H. R. 1969, Sol. Phys., 10, 79
Bulanov, S. V., & Sakai, J.-I. 1998, ApJS, 117, 599
Chae, J., Wang, H., Lee, C.-Y., Goode, P. R., & Schuehle, U. 1998, ApJ, 497, L109
Chen, P. F., Fang, C., & Ding, M. D. 2001, Chin. J. Astron. Astrophys., 1, 176
Chen, Q. R., & Ding, M. D. 2006, ApJ, 641, 1217
Christe, S., Hannah, I. G., Krucker, S., McTiernan, J., & Lin, R. P. 2008, ApJ, 677, 1385
Crockett, P. J., Jess, D. B., Mathioudakis, M., & Keenan, F. P. 2009, MNRAS, 397, 1852
Denker, C. 1997, A&A, 323, 599
Denker, C., de Boer, C. R., Volkmer, R., & Kneer, F. 1995, A&A, 296, 567
Dere, K. P. 1994, Adv. Space Res., 14, 13
Ding, M. D., Chen, Q. R., Li, J. P., & Chen, P. F. 2003, ApJ, 598, 683
Ding, M. D., Fang, C., & Huang, Y. R. 1995, Sol. Phys., 158, 81
Ding, M. D., Fang, C., & Yun, H. S. 1999, ApJ, 512, 454
Ellerman, F. 1917, ApJ, 46, 298
Emslie, A. G., Brown, J. C., & Machado, M. E. 1981, ApJ, 246, 337
Georgoulis, M. K., Rust, D. M., Bernasconi, P. N., & Schmieder, B. 2002, ApJ, 575, 506
Hannah, I. G., Christe, S., Krucker, S., Hurford, G. J., Hudson, H. S., & Lin, R. P. 2008, ApJ, 677, 704
Hudson, H. S. 1991, Sol. Phys., 133, 357
Jain, R., Browning, P., & Kusano, K. 2005, Phys. Plasmas, 12, 012904
Jess, D. B., Mathioudakis, M., Crockett, P. J., & Keenan, F. P. 2008, ApJ, 688, L119
Jess, D. B., McAteer, R. T. J., Mathioudakis, M., Keenan, F. P., Andic, A., & Bloomfield, D. S. 2007, A&A, 476, 971
Krucker, S., Christe, S., Lin, R. P., Hurford, G. J., & Schwartz, R. A. 2002, Sol. Phys., 210, 445
Litvinenko, Y. E. 1999, ApJ, 515, 435
Litvinenko, Y. E., Chae, J., & Park, S.-Y. 2007, ApJ, 662, 1302
Litvinenko, Y. E., & Martin, S. F. 1999, Sol. Phys., 190, 45
Ma, Z. W., Wang, X., & Bhattacharjee, A. 1996, Phys. Plasmas, 3, 2427
Machado, M. E., Emslie, A. G., & Avrett, E. H. 1989, Sol. Phys., 124, 303
Madjarska, M. S., Doyle, J. G., & de Pontieu, B. 2009, ApJ, 701, 253
Nindos, A., & Zirin, H. 1998, Sol. Phys., 182, 381
Priest, E. R. 1986, Adv. Space Res., 6, 73
Qiu, J., Ding, M. D., Wang, H., Denker, C., & Goode, P. R. 2000, ApJ, 544, L157
Roumeliotis, G., & Moore, R. L. 1993, ApJ, 416, 386
Sanchez Almeida, J., & Martinez Pillet, V. 1994, ApJ, 424, 1014
Scherrer, P. H., et al. 1995, Sol. Phys., 162, 129
Spitzer, L. 1956, Physics of Fully Ionized Gases (New York: Interscience)
Suematsu, Y., Wang, H., & Zirin, H. 1995, ApJ, 450, 411
Vekstein, G., & Bian, N. 2005, ApJ, 632, L151
Vekstein, G. E., & Jain, R. 1998, Phys. Plasmas, 5, 1506
Vernazza, J. E., Avrett, E. H., & Loeser, R. 1981, ApJS, 45, 635
Wang, X., Ma, Z. W., & Bhattacharjee, A. 1996, Phys. Plasmas, 3, 2129
Zachariadis, T. G., Alissandrakis, C. E., & Banos, G. 1987, Sol. Phys., 108, 227